

# Krylov Projection Framework for Fourier Model Reduction <sup>★</sup>

Serkan Gugercin <sup>a</sup>, Karen Willcox <sup>b</sup>

<sup>a</sup>*Department of Mathematics, Virginia Tech, 442 McBryde Hall, Blacksburg, VA, 24061-0123*

<sup>b</sup>*Department of Aeronautics and Astronautics, MIT, 77 Massachusetts Avenue, Room 37-447, Cambridge, MA 02143, USA*

---

## Abstract

This paper analyzes the Fourier model reduction (**FMR**) method from a rational Krylov projection framework and shows how the **FMR** reduced model, which has guaranteed stability and a global error bound, can be computed in a numerically efficient and robust manner. By monitoring the rank of the Krylov subspace that underlies the **FMR** model, the projection framework also provides an improved criterion for determining the number of Fourier coefficients that are needed, and hence the size of the resulting reduced-order model. The advantages of applying **FMR** in the rational Krylov projection framework are demonstrated on a simple example.

*Key words:* Model reduction; system order reduction

---

## 1 Introduction

Model reduction entails the systematic generation of cost-efficient representations of large-scale systems that result, for example, from discretization of partial differential equations (PDEs). Recent years have seen the development of several reduction methods that are computationally tractable for large-scale systems. These methods have been applied in many different settings with considerable success, including controls, fluid dynamics, structural dynamics, and circuit design.

Algorithms such as optimal Hankel model reduction [1,3,15,8] and balanced truncation [20,19] come with rigorous guarantees of quality and global error bounds on the resulting reduced models. These methods are usually referred to as singular value decomposition (SVD) or gramian-based model reduction methods. Despite their appealing theoretical properties, the computational requirements associated with these methods make them impractical for application to large-scale systems of order  $10^5$  or higher. Several other methods have been developed that are applicable to large-scale systems, including Krylov-based methods [9,5,7], approximate balanced truncation [11,17], and proper orthogonal de-

composition (POD) [14,22,16]. In many cases, this latter group of methods trades computational efficiency for a lack of rigorous guarantees and global error bounds.

A lack of guarantees on the stability of the reduced model is one problem often encountered when using Krylov- or POD-based reduction methods. In particular, a tendency of these methods to produce unstable models has been noted for applications in computational fluid dynamics using the Euler equations [23]. For Krylov-based reduction methods, different approaches have been proposed to resolve the stability issue. The implicit restart algorithm proposed by Grimme *et al.* [10] guarantees stability by removing the unstable reduced poles through an implicitly restarted Lanczos algorithm. However, the stability comes at the cost that the reduced model is no longer an exact interpolant of the original model, but of a near-by perturbed model. On the other hand, Fourier model reduction (**FMR**) [23] of Willcox and Megretski preserves stability by first performing a bilinear transformation and then applying model reduction in the discrete-frequency domain via a truncated Fourier expansion. Similar to **FMR**, to guarantee stability, Least-squares model reduction method [12] of Gugercin and Antoulas uses a bilinear transformation. Then, model reduction is performed in discrete-time in a different way by combining SVD and Krylov-based methods.

Despite its theoretical properties such as guaranteed stability and a global error bound, and its success in yielding good reduced models [23], the underlying projec-

---

<sup>★</sup> This paper was not presented at any IFAC meeting. Corresponding author K. Willcox. Tel. +1-617-253-3503. Fax +1-617-258-5143.

*Email addresses:* [gugercin@math.vt.edu](mailto:gugercin@math.vt.edu) (Serkan Gugercin), [kwillcox@mit.edu](mailto:kwillcox@mit.edu) (Karen Willcox).

tion framework and Krylov-based (interpolation) features of FMR have gone unnoticed. This paper analyzes the **FMR** method from a projection framework and shows the underlying rational Krylov projection behind **FMR**. Through this analysis, we illustrate the interpolation and restricted optimal  $\mathcal{H}_2$  properties of **FMR**; and show how the **FMR** reduced model can be computed in a numerically efficient and robust manner in a Krylov-based model reduction setting. Moreover, a new, more robust stopping criterion for **FMR** is proposed.

The remainder of the paper is organized as follows: In Section 2, model reduction via projection is described. In Section 3, a brief description of the **FMR** method is presented. Interpolation and optimality properties of the method are discussed in Section 4. Section 5 presents the rational Krylov projection framework, and global error expressions and error bounds. Results for numerical experiments are presented in Section 6.

## 2 Model Reduction via Projection

Consider a single-input/single-output (SISO) dynamical system  $\mathbf{G}(s)$  with transfer function

$$\mathbf{G}(s) = \mathbf{h}(s\mathbf{I} - \mathbf{F})^{-1}\mathbf{g} + \mathbf{J}, \quad (1)$$

where  $\mathbf{F} \in \mathbb{R}^{n \times n}$ ,  $\mathbf{g}, \mathbf{h}^T \in \mathbb{R}^n$ , and  $\mathbf{J} \in \mathbb{R}$ . The goal of model reduction, in this setting, is to produce a much smaller order system  $\mathbf{G}_r(s)$  with transfer function

$$\mathbf{G}_r(s) = \mathbf{h}_r(s\mathbf{I}_r - \mathbf{F}_r)^{-1}\mathbf{g}_r + \mathbf{J}_r, \quad (2)$$

where  $\mathbf{F}_r \in \mathbb{R}^{r \times r}$ ,  $\mathbf{g}_r, \mathbf{h}_r^T \in \mathbb{R}^r$ , and  $\mathbf{J}_r \in \mathbb{R}$ , such that the reduced system  $\mathbf{G}_r(s)$  approximates  $\mathbf{G}(s)$  well. In *model reduction via projection*,  $\mathbf{G}_r(s)$  in (2) is obtained as

$$\mathbf{F}_r = \mathbf{W}^T \mathbf{F} \mathbf{V}, \quad \mathbf{g}_r = \mathbf{W}^T \mathbf{g}, \quad \mathbf{h}_r = \mathbf{h} \mathbf{V}, \quad \text{and} \quad \mathbf{J}_r = \mathbf{J}, \quad (3)$$

where  $\mathbf{V} \in \mathbb{R}^{n \times r}$  and  $\mathbf{W} \in \mathbb{R}^{n \times r}$  with  $\mathbf{W}^T \mathbf{V} = \mathbf{I}_r$ . The corresponding oblique projector is given by  $\mathbf{V} \mathbf{W}^T$ . Since  $\mathbf{J}_r = \mathbf{J}$ , without loss of generality, we assume that  $\mathbf{J} = 0$

### 2.1 Rational Krylov based model reduction

In model reduction by rational Krylov projection, the goal is to find a reduced model  $\mathbf{G}_r(s)$  as in (2) and (3) that interpolates  $\mathbf{G}(s)$  and a certain number of its derivatives (called moments) at selected points  $s_k$  in the complex plane. In other words, the goal is to find the reduced system matrices  $\mathbf{F}_r$ ,  $\mathbf{g}_r$ , and  $\mathbf{h}_r$  so that

$$\begin{aligned} \left. \frac{(-1)^j}{j!} \frac{d^j \mathbf{G}(s)}{ds^j} \right|_{s=s_k} &= \mathbf{h}(s_k \mathbf{I}_n - \mathbf{F})^{-(j+1)} \mathbf{g} \\ &= \mathbf{h}_r (s_k \mathbf{I}_r - \mathbf{F}_r)^{-(j+1)} \mathbf{g}_r = \left. \frac{(-1)^j}{j!} \frac{d^j \mathbf{G}_r(s)}{ds^j} \right|_{s=s_k} \end{aligned} \quad (4)$$

for  $k = 1, \dots, K$  and for  $j = 1, \dots, J$  where  $K$  and  $J$  denote, respectively, the number of interpolation points  $s_k$  and the number of moments to be matched at each  $s_k$ . The quantity  $\mathbf{h}(s_k \mathbf{I}_n - \mathbf{F})^{-(j+1)} \mathbf{g}$  is the  $j^{\text{th}}$  moment of  $\mathbf{G}(s)$  at  $s_k$ . If  $s_k = \infty$ , the moments are called Markov parameters and are given by  $\mathbf{h} \mathbf{F}^j \mathbf{g}$  for  $j = 0, 1, 2, \dots$ . Since the moments are extremely ill-conditioned to compute, the goal in rational Krylov-based model reduction is to find  $\mathbf{G}_r(s)$  that satisfies (4) *without computing the moments explicitly*. Skelton *et al.* in [4,24] showed that the matrices  $\mathbf{V}$  and  $\mathbf{W}$  chosen so that

$$\begin{aligned} \text{Ran}(\mathbf{V}) &= \text{Im}\{(s_1 \mathbf{I} - \mathbf{F})^{-1} \mathbf{g}, \dots, (s_1 \mathbf{I} - \mathbf{F})^{-K_1} \mathbf{g}, \\ &\quad \dots, (s_J \mathbf{I} - \mathbf{F})^{-1} \mathbf{g}, \dots, (s_J \mathbf{I} - \mathbf{F})^{-K_J} \mathbf{g}\} \\ \text{Ran}(\mathbf{W}) &= \text{Im}\{(\overline{s_1} \mathbf{I} - \mathbf{F}^T)^{-1} \mathbf{h}^T, \dots, (\overline{s_1} \mathbf{I} - \mathbf{F}^T)^{-K_1} \mathbf{h}^T, \\ &\quad \dots, (\overline{s_J} \mathbf{I} - \mathbf{F}^T)^{-1} \mathbf{h}^T, \dots, (\overline{s_J} \mathbf{I} - \mathbf{F}^T)^{-K_J} \mathbf{h}^T\}, \end{aligned}$$

produce reduced-order models  $\mathbf{G}_r(s)$  via (3) matching  $2K_i$  moments of  $\mathbf{G}(s)$  at the interpolation points  $s_i$  for  $i = 1, \dots, J$ , i.e.  $\mathbf{G}_r(s)$  interpolates  $\mathbf{G}(s)$  and its first  $2K_i - 1$  derivatives at each  $s_i$ ; hence matching the moments without ever computing them. Grimme [9] showed how one can obtain the required matrices  $\mathbf{V}$  and  $\mathbf{W}$  as above in a numerically efficient way using the rational Krylov method of Ruhe [21], and hence showed how to solve moment matching problem using *Krylov projection* methods in an effective way.

## 3 Fourier Model Reduction

Given  $\mathbf{G}(s)$  as in (1), let the  $n^{\text{th}}$ -order discrete-time system

$$\mathbf{H}(z) = \mathbf{c}(z\mathbf{I} - \mathbf{A})^{-1}\mathbf{b} + \mathbf{d}$$

be obtained from  $\mathbf{G}(s)$  via a bilinear transformation, i.e.

$$\begin{aligned} \mathbf{A} &= (\omega_0 \mathbf{I} + \mathbf{F})(\omega_0 \mathbf{I} - \mathbf{F})^{-1}, \quad \mathbf{b} = \sqrt{2\omega_0} (\omega_0 \mathbf{I} - \mathbf{F})^{-1} \mathbf{g}, \\ \mathbf{c} &= \sqrt{2\omega_0} \mathbf{h} (\omega_0 \mathbf{I} - \mathbf{F})^{-1}, \quad \mathbf{d} = \mathbf{J} + \mathbf{h} (\omega_0 \mathbf{I} - \mathbf{F})^{-1} \mathbf{g}, \end{aligned}$$

where  $\omega_0 > 0$ . It is well known that

$$\mathbf{G}(s) = \mathbf{H}\left(\frac{\omega_0 + s}{\omega_0 - s}\right) \quad \text{or} \quad \mathbf{G}\left(\omega_0 \frac{z-1}{z+1}\right) = \mathbf{H}(z). \quad (5)$$

Let  $\eta_i$  denote the Markov parameters of the discrete-time system  $\mathbf{H}(z)$ ,

$$\eta_0 = \mathbf{d}, \quad \text{and} \quad \eta_i = \mathbf{c} \mathbf{A}^{i-1} \mathbf{b}, \quad i \geq 1. \quad (6)$$

**FMR** was proposed in [23] as an efficient method to compute reduced models with guaranteed stability and a rigorous error bound. **FMR** uses discrete-time Fourier coefficients to compute an intermediate discrete-time reduced model, to which balanced truncation can be

subsequently applied using explicit formulae. The  $r^{\text{th}}$ -order intermediate reduced model  $\mathbf{H}_r(z) = \mathbf{c}_r(z\mathbf{I}_r - \mathbf{A}_r)^{-1}\mathbf{b}_r + \mathbf{d}$  is defined by

$$\mathbf{H}_r(z) = \sum_{k=0}^r \eta_k z^{-k}, \quad (7)$$

and has the form

$$\begin{aligned} \mathbf{A}_r &= [\mathbf{e}_2, \mathbf{e}_3, \dots, \mathbf{e}_r, \mathbf{0}], & \mathbf{b}_r &= \mathbf{e}_1, \\ \mathbf{c}_r &= [\eta_1, \eta_2, \dots, \eta_r], & \mathbf{d}_r &= \eta_0, \end{aligned} \quad (8)$$

where  $\mathbf{e}_i$  denotes the  $i^{\text{th}}$  unit vector and  $\mathbf{0}$  is a vector of zeroes. If desired, a continuous-time reduced model  $\mathbf{G}_r(s)$  can be obtained from  $\mathbf{H}_r(z)$  by an inverse bilinear transformation. As shown in [23], both the intermediate discrete-time model  $\mathbf{H}_r(z)$  and the final continuous-time reduced model  $\mathbf{G}(s)$  are stable. Moreover, let  $\mathbf{E}(z) := \mathbf{H}(z) - \mathbf{H}_r(z)$  be the discrete-time error system. Then,

$$\|\mathbf{E}(z)\|_{\mathcal{H}_\infty}^2 \leq \frac{r^{1-2q}}{2\pi(2q-1)} \int_{-\pi}^{\pi} \left| \mathbf{H}^{(q)}(e^{j\theta}) \right|^2 d\theta, \quad (9)$$

where  $\mathbf{H}^{(q)}$  is the  $q^{\text{th}}$  derivative of  $\mathbf{H}(e^{j\theta})$  with respect to  $\theta$ .

For the rest of the paper,  $\mathbf{H}(z)$  denotes the discrete-time system in (5) obtained via bilinear transformation of  $\mathbf{G}(s)$ .  $\mathbf{H}_r(z)$  denotes the intermediate reduced-order model as in (7) and (8) obtained from  $\mathbf{H}(z)$  via FMR. Finally,  $\mathbf{G}_r(s)$  is final continuous-time reduced system obtained via inverse bilinear transformation of  $\mathbf{H}_r(z)$ .

#### 4 Interpolation and Optimality Properties of FMR and $\mathcal{H}_2/\mathcal{H}_\infty$ error bounds

**Lemma 1**  $\mathbf{H}_r(z)$  matches the first  $r$  Markov parameters of  $\mathbf{H}(z)$ . Hence,  $\mathbf{G}_r(s)$  interpolates the first  $r$  moments of  $\mathbf{G}(s)$  at  $s = \omega_0$ .

**Proof:** The first part of the lemma follows from the construction of  $\mathbf{H}_r(z)$  in (7) and (8). The second part follows from combining this result with (5) and by taking successive derivatives of (5).  $\square$

**Lemma 2**  $\mathbf{H}_r(z)$  is the  $r^{\text{th}}$ -order optimal  $\mathcal{H}_2$  approximation to  $\mathbf{H}(z)$  among all models having all  $r$  poles located at  $z = 0$ . In other words, define

$$\tilde{\mathbf{H}}(z) = \mathbf{d} + \frac{\beta_1 z^{r-1} + \beta_2 z^{r-2} + \dots + \beta_{r-1} z^{r-1}}{z^r}.$$

Then,  $\mathbf{H}_r(z) = \arg \min_{\mathbf{n}(z)} \|\mathbf{H} - \tilde{\mathbf{H}}\|_{\mathcal{H}_2}$ .

The following theorem, slightly modified from [18,6], is used in proving Lemma 2.

**Theorem 3** [18,6] Given a stable discrete-time dynamical  $\mathbf{H}(z) = \mathbf{c}(z\mathbf{I} - \mathbf{A})^{-1} + \mathbf{d}$ , and a fixed stable pole  $\alpha$ , define  $\hat{\mathbf{H}}_r(z) := \mathbf{d} + \frac{\beta_0 + \beta_1 z + \dots + \beta_{r-1} z^{r-1}}{(z - \alpha)^r}$ . Then

$\|\mathbf{H} - \hat{\mathbf{H}}_r\|_{\mathcal{H}_2}$  is minimized if and only if

$$\frac{d^j \mathbf{H}(z)}{dz^j} = \frac{d^j \hat{\mathbf{H}}_r(z)}{dz^j} \text{ at } z = \frac{1}{\alpha}, \text{ for } j = 0, \dots, r-1. \quad (10)$$

**Proof of Lemma 2:** It follows from (8) that  $\mathbf{H}_r(z)$  has all of its poles located at  $z = 0$ . Hence, due to Theorem 3, what remains to show is that  $\mathbf{H}_r(z)$  satisfies (10) for  $z = \infty$ . However, this is true as shown in Lemma 1;  $\mathbf{H}_r(z)$  interpolates first  $r$  moments of  $\mathbf{H}(z)$  at  $z = \infty$ , i.e. the first  $r$  Markov parameters.  $\square$

**Lemma 4** Given the above set-up,

$$\|\mathbf{H}(z) - \mathbf{H}_r(z)\|_{\mathcal{H}_2} = \sum_{i=r+1}^{\infty} |\eta_i|^2. \quad (11)$$

Moreover, let  $\mathbf{A}$  be diagonalizable and let  $\mathbf{A} = \mathbf{U}\mathbf{\Lambda}\mathbf{U}^{-1}$  be the eigenvalue decomposition with  $\mathbf{\Lambda} = \text{diag}(\lambda_1, \dots, \lambda_n)$ . Define  $\kappa_{\mathbf{A}} = \|\mathbf{U}\| \|\mathbf{U}^{-1}\|$  and  $\rho_{\mathbf{A}} = \max_i |\lambda_i|$ . Then

$$\|\mathbf{H}(z) - \mathbf{H}_r(z)\|_{\mathcal{H}_2} \leq \|\mathbf{c}\|^2 \|\mathbf{b}\|^2 \kappa_{\mathbf{A}}^2 \frac{\rho_{\mathbf{A}}^{2r}}{1 - \rho_{\mathbf{A}}^2}. \quad (12)$$

**Proof:** (11) follows from the fact that by definition of  $\mathbf{H}_r(z)$  in (7),  $\mathbf{H}(z) - \mathbf{H}_r(z) = \sum_{k=r+1}^{\infty} \eta_k z^{-k}$ . To prove (12), first use the definition of  $\eta_i = \mathbf{c}\mathbf{A}^{i-1}\mathbf{b}$  in (7) and note that  $|\eta_i|^2 \leq \|\mathbf{c}\|^2 \|\mathbf{b}\|^2 \|\mathbf{A}^{i-1}\|^2$ . Plugging  $\mathbf{A} = \mathbf{U}\mathbf{\Lambda}\mathbf{U}^{-1}$  into the last inequality and using  $\|\mathbf{A}\| \leq \|\mathbf{U}\| \|\mathbf{\Lambda}\| \|\mathbf{U}^{-1}\|$  leads to the desired formula (12) after realizing  $\|\mathbf{\Lambda}\| = \rho_{\mathbf{A}} < 1$ .  $\square$

**Remark 5** Note that (11) is a global error expression, and does not involve reduced-order matrices. Since  $\rho_{\mathbf{A}} < 1$ , for sufficiently large values of  $i$ ,  $\eta_i^2$  will decrease quickly. We note that even though (11) contains an infinite sum, since  $\eta_i = \mathbf{c}\mathbf{A}^{i-1}\mathbf{b}$  and  $\rho_{\mathbf{A}} < 1$ , it is always bounded as shown in (12). This behavior is similar to the decay of Hankel singular values and the error bound (11) has a similar structure to that in the balanced truncation framework. On the other hand, (12) gives an a priori global error bound, which can be easily computable for small-to-medium scale problems.

**Corollary 6** For  $q = 1, 2, \dots$ ,

$$\|\mathbf{G}(s) - \mathbf{G}_r(s)\|_{\mathcal{H}_\infty}^2 \leq \frac{r^{1-2q}}{2\pi(2q-1)} \int_{-\pi}^{\pi} \left| \mathbf{H}^{(q)}(e^{j\theta}) \right|^2 d\theta,$$

where  $\mathbf{H}^{(q)}$  is the  $q^{\text{th}}$  derivative of  $\mathbf{H}(e^{j\theta})$  with respect to  $\theta$ .

**Proof:** The result follows from combining (9) with the fact that bilinear transformation preserves the  $\mathcal{H}_\infty$  norm.  $\square$

**Remark 7** If the derivatives  $\mathbf{H}^{(q)}$  can be computed using some quadrature rule, then Corollary 6 provides a computable  $\mathcal{H}_\infty$  error bound for the continuous-time error system.

## 5 Rational Krylov Projection Framework for FMR

In this section, we analyze **FMR** from a (rational Krylov) projection framework and derive an algorithm that constructs  $\mathbf{H}_r(z)$  in (8) from  $\mathbf{H}(z)$  using a Krylov-based algorithm without directly computing the Markov parameters  $\eta_i$ . The motivation for this analysis is twofold. First, in the case where the spectral radius of  $\mathbf{A}$  is close to unity, the Krylov-based approach provides a numerically more robust way to compute the **FMR** reduced model. Second, in [23] it was proposed that magnitudes of the Markov parameters should be used as a guidance to select  $r$ , the size of the **FMR** reduced model. We will show that the Krylov approach provides a better way to determine an appropriate value of  $r$ .

### 5.1 Projection matrices

To derive the rational Krylov framework for **FMR**, we must construct matrices  $\mathbf{V}$  and  $\mathbf{W}$  where  $\mathbf{V}$  and/or  $\mathbf{W}$  span a Krylov subspace with  $\mathbf{W}^T \mathbf{V} = \mathbf{I}_r$  such that the projections

$$\mathbf{A}_r = \mathbf{W}^T \mathbf{A} \mathbf{V}, \quad \mathbf{b}_r = \mathbf{W}^T \mathbf{b}, \quad \mathbf{c}_r = \mathbf{c} \mathbf{V} \quad (13)$$

yield the matrices in (8). Since  $\mathbf{H}_r(z)$  matches the first  $r$  Markov parameters of  $\mathbf{H}(z)$ , it follows that the matrix  $\mathbf{V}$  is given by

$$\mathbf{V} = [\mathbf{b}, \mathbf{A}\mathbf{b}, \mathbf{A}^2\mathbf{b}, \dots, \mathbf{A}^{r-1}\mathbf{b}]. \quad (14)$$

Eq. (14) shows that  $\mathbf{V}$  spans a regular Krylov subspace, hence reflecting the underlying Krylov projection framework for **FMR**. Next, we need to determine  $\mathbf{W}$ . Let  $\mathbf{W}$  be **any** left inverse of  $\mathbf{V}$ . Since  $\mathbf{W}^T \mathbf{V} = \mathbf{I}_r$ , one has

$$[\mathbf{W}^T \mathbf{b}, \mathbf{W}^T \mathbf{A}\mathbf{b}, \mathbf{W}^T \mathbf{A}^2\mathbf{b}, \dots, \mathbf{W}^T \mathbf{A}^{r-1}\mathbf{b}] = \mathbf{I}_r,$$

or equivalently  $\mathbf{W}^T \mathbf{A}^{i-1} \mathbf{b} = \mathbf{e}_i$ ,  $i = 1, \dots, r$ . For this selection of  $\mathbf{W}$ , the resulting reduced system matrices are given by

$$\begin{aligned} \mathbf{A}_r &= \mathbf{W}^T \mathbf{A} \mathbf{V} = \mathbf{W}^T [\mathbf{A}\mathbf{b}, \mathbf{A}^2\mathbf{b}, \dots, \mathbf{A}^r \mathbf{b}] \\ &= [\mathbf{e}_2, \mathbf{e}_3, \dots, \mathbf{e}_r, \mathbf{W}^T \mathbf{A}^r \mathbf{b}], \end{aligned} \quad (15)$$

$$\mathbf{b}_r = \mathbf{W}^T \mathbf{b} = \mathbf{e}_1, \quad \text{and} \quad \mathbf{c}_r = \mathbf{c} \mathbf{V} = [\eta_1, \eta_2, \dots, \eta_r]. \quad (16)$$

As can be seen from (16),  $\mathbf{b}_r$  and  $\mathbf{c}_r$  are already in the desired form (8) for **any** left inverse  $\mathbf{W}$  of  $\mathbf{V}$ . Also, (15) shows that the first  $r-1$  columns of  $\mathbf{A}_r$  have the desired form. In order to achieve the appropriate last column of  $\mathbf{A}_r$  as in (8), we require  $\mathbf{W}$  to satisfy

$$\mathbf{W}^T \mathbf{V} = \mathbf{I}_r \quad \text{and} \quad \mathbf{W}^T \mathbf{A}^r \mathbf{b} = \mathbf{0}.$$

The following lemma specifies this selection of  $\mathbf{W}$ :

**Lemma 8** Let  $\mathbf{V}$  be as given in (14). Moreover, let

$$[\mathbf{V} \quad \mathbf{A}^r \mathbf{b}] = [\mathbf{Q}_1 \quad \mathbf{q}_2] \begin{bmatrix} \mathbf{R}_1 & \mathbf{x} \\ \mathbf{0} & \alpha \end{bmatrix} \quad (17)$$

be the QR-decomposition of  $[\mathbf{V} \quad \mathbf{A}^r \mathbf{b}]$ , i.e.  $\mathbf{Q}_1^T \mathbf{Q}_1 = \mathbf{I}_r$ ,  $\mathbf{q}_2^T \mathbf{q}_2 = 1$ ,  $\mathbf{Q}_1^T \mathbf{q}_2 = \mathbf{0}$ , and  $\mathbf{R}_1$  is an upper-triangular matrix. Then, using

$$\mathbf{W} = (\mathbf{Q}_1 - \frac{1}{\alpha} \mathbf{q}_2 \mathbf{x}^T) \mathbf{R}_1^{-T} \quad (18)$$

together with  $\mathbf{V}$  in the projection (13) yields the desired reduced-order matrices in (8).

**Proof:** If we only required  $\mathbf{W}$  to be a left inverse of  $\mathbf{V}$ , a straightforward choice would be  $\mathbf{W}^T = \mathbf{R}_1^{-1} \mathbf{Q}_1^T$ . However, to force the additional constraint  $\mathbf{W}^T \mathbf{A}^r \mathbf{b} = \mathbf{0}$ , this selection must be modified so that the left inverse property still holds with the additional property that  $\mathbf{A}^r \mathbf{b}$  is in the kernel of  $\mathbf{W}^T$ . To achieve this, one needs to use the QR-decomposition of the appended matrix  $[\mathbf{V} \quad \mathbf{A}^r \mathbf{b}]$ . From (17), a potential selection is of the form

$$\mathbf{W}^T = \mathbf{R}_1^{-1} (\mathbf{Q}_1^T + \mathbf{z} \mathbf{q}_2^T). \quad (19)$$

We observe that this selection still satisfies  $\mathbf{W}^T \mathbf{V} = \mathbf{0}$ . So, what is left is to find the appropriate  $\mathbf{z}$  so that  $\mathbf{W}^T \mathbf{A}^r \mathbf{b} = \mathbf{0}$ . It follows from (17) that  $\mathbf{A}^r \mathbf{b} = \mathbf{Q}_1 \mathbf{x} + \mathbf{q}_2 \alpha$ . Plugging this expression, together with  $\mathbf{W}^T$  as in (19), into the equation  $\mathbf{W}^T \mathbf{A}^r \mathbf{b} = \mathbf{0}$  and solving for  $\mathbf{z}$  yields the solution  $\mathbf{z} = -\frac{1}{\alpha} \mathbf{x}$ . Finally, using this selection of  $\mathbf{z}$  in (19) completes the proof.  $\square$

**Remark 9** The formulation in Lemma 8 puts **FMR** into a rational Krylov projection framework: one simply uses an Arnoldi-type algorithm to compute an orthogonal basis for  $[\mathbf{V} \quad \mathbf{A}^r \mathbf{b}] = [\mathbf{b}, \mathbf{A}\mathbf{b}, \mathbf{A}^2\mathbf{b}, \dots, \mathbf{A}^r \mathbf{b}]$ , which spans a Krylov subspace. Even though the required subspace is a regular Krylov subspace in terms of the discrete-time matrices, it is a rational Krylov subspace in terms of the original continuous-time matrices. However, only one shift has been used, and hence only one sparse decomposition is required. Hence, this formulation of **FMR** can be implemented in a numerically effective way. As noted above, direct computation of the Markov parameters is avoided.

**Remark 10** In a systems theoretical setting, going from  $\mathbf{H}(z)$  to  $\mathbf{H}_r(z)$  amounts to direct truncation of the controllable canonical form of  $\mathbf{H}(z)$ . Let  $\mathcal{Q}$  be the full controllability matrix for  $\mathbf{H}(z)$ , i.e.  $\mathcal{Q} = [\mathbf{b}, \mathbf{A}\mathbf{b}, \dots, \mathbf{A}^{n-1}\mathbf{b}]$ . Then, the projection (13) amounts to choosing  $\mathbf{V}$  as the first  $r$  columns of  $\mathcal{Q}$  and  $\mathbf{W}^T$  as the first  $r$  rows of  $\mathcal{Q}^{-1}$ .

## 5.2 Computational implementation

Even though the above analysis puts **FMR** into Krylov projection framework, it uses the power basis  $\mathbf{V}$  explicitly, which is numerically ill-conditioned. Here, we will resolve this issue and show how to avoid explicit computation of  $\mathbf{V}$  while still obtaining the quantities  $\mathbf{R}_1, \mathbf{x}$  and  $\alpha$  that result from the QR-decomposition of  $\mathbf{V}$  as defined in (17).

One can show that

$$\mathbf{A}[\mathbf{V} \ \mathbf{A}^r \mathbf{b}] = [\mathbf{V} \ \mathbf{A}^r \mathbf{b}] [\mathbf{e}_2, \mathbf{e}_3 \dots \mathbf{e}_{r+1}, \mathbf{h}_{r+1}] + \mathbf{f} \mathbf{e}_{r+1}^T, \quad (20)$$

where  $\mathbf{h}_{r+1}$  and  $\mathbf{f}$  are vectors of appropriate size. Based on (17) and (20), we make the following definitions:

$$\mathbf{Q} := [\mathbf{Q}_1 \ \mathbf{q}_2], \quad \mathbf{R} := \begin{bmatrix} \mathbf{R}_1 & \mathbf{x} \\ \mathbf{0} & \alpha \end{bmatrix},$$

$$\mathbf{H} := [\mathbf{e}_2, \mathbf{e}_3 \dots \mathbf{e}_{r+1}, \mathbf{h}_{r+1}]. \quad (21)$$

Therefore, (20) becomes  $\mathbf{AQR} = \mathbf{QRH} + \mathbf{f} \mathbf{e}_{r+1}^T$ . Multiplying this expression by  $\mathbf{R}^{-1}$  from right, we obtain

$$\mathbf{AQ} = \underbrace{\mathbf{QRHR}^{-1}}_{:=\hat{\mathbf{H}}} + \underbrace{\mathbf{f} \mathbf{e}_{r+1}^T \mathbf{R}^{-1}}_{:=\hat{\mathbf{f}} \mathbf{e}_{r+1}^T}, \quad (22)$$

$$\text{i.e. } \mathbf{AQ} = \mathbf{Q}\hat{\mathbf{H}} + \hat{\mathbf{f}} \mathbf{e}_{r+1}^T. \quad (23)$$

Eq. (23) is precisely what one would obtain if  $r+1$  steps of the Arnoldi algorithm were run on  $\mathbf{A}$  and  $\mathbf{b}$ . This is done without explicitly forming the powers of  $\mathbf{A}$ . However, to obtain the desired matrix  $\mathbf{W}$  in (18), we need to **extract**  $\mathbf{R}$  from  $\hat{\mathbf{H}}$ . Because of the specific upper Hessenberg structures of  $\mathbf{H}$  and  $\hat{\mathbf{H}}$ , this can be done as follows. Note that, by definition,

$$\hat{\mathbf{H}}\mathbf{R} = \mathbf{R}\mathbf{H}. \quad (24)$$

Let  $\hat{h}_{ij}$  and  $\rho_{ij}$  denote the  $(i, j)$ <sup>th</sup> entry of  $\hat{\mathbf{H}}$  and  $\mathbf{R}$ , respectively. Also, let  $\hat{\mathbf{h}}_j$  and  $\mathbf{r}_j$  denote, respectively, the  $j$ <sup>th</sup> columns of  $\hat{\mathbf{H}}$  and  $\mathbf{R}$ .  $\mathbf{r}_1$  is explicitly known:  $\mathbf{r}_1 = \|\mathbf{b}\| \mathbf{e}_1$  (hence,  $\rho_{11} = \|\mathbf{b}\|$ ). Multiplying (24) with  $\mathbf{e}_1$  from the left yields  $\rho_{11} \hat{\mathbf{h}}_1 = \mathbf{r}_2$ ; hence, the second column of  $\mathbf{R}$  is obtained. Then, similarly, multiplication by  $\mathbf{e}_2$  yields  $\mathbf{r}_3$ , and so on. Continuing in this way,

one **extracts**  $\mathbf{R}$  from  $\hat{\mathbf{H}}$  iteratively *without forming*  $\mathbf{V}$  as desired. This approach of obtaining  $\mathbf{R}$  is numerically efficient since it only requires  $r$  matrix-vector multiplications with the small matrix  $\hat{\mathbf{H}} \in \mathbb{R}^{(r+1) \times (r+1)}$ . Moreover, the vector multiplying the matrix  $\hat{\mathbf{H}}$  at the  $k$ <sup>th</sup> step has only  $k$  non-zero entries. Upon completion of the iterative process, one can construct the required reduced model by re-defining  $\mathbf{V}$  and  $\mathbf{W}$  as

$$\mathbf{V} = \mathbf{Q}_1 \quad \text{and} \quad \mathbf{W} = \mathbf{Q}_1 - \frac{1}{\alpha} \mathbf{q}_2 \mathbf{x}^T, \quad (25)$$

without forming the power basis. The resulting reduced-model will have the same transfer function  $\mathbf{H}_r(z)$  as in (7) as desired and be only a similarity transformation away from the state-space matrices in (8). (25) completes the effective numerical computation of **FMR** through rational Krylov projection. As explained above, this is achieved by first running  $r+1$  steps of Arnoldi algorithm on  $\mathbf{A}$  and  $\mathbf{b}$ , then extracting  $\mathbf{R}$  from the Arnoldi basis and finally reducing the system via projection using  $\mathbf{V}$  and  $\mathbf{W}$  in (25).

## 5.3 A stopping criterion for **FMR**

Ref. [23] proposed that magnitudes of the Markov parameters should be used as a guidance to select  $r$ , the size of the **FMR** reduced model. Even though this approach works effectively for the cases where the magnitudes of the Markov parameters  $\eta_i$  decrease rapidly, it might lead to unnecessarily large reduced-order dimension  $r$  when the  $\eta_i$  decrease very slowly. This can be explained by observing that even if the magnitudes of the Markov parameters are not decreasing, the Krylov subspace  $\mathbf{V}$  underlying **FMR** will *not* necessarily carry new information with the addition of another column; in other words, even though the  $\eta_i$  are not decreasing, it is possible that the Krylov subspace  $\mathbf{V}$  is almost rank deficient and another column does *not* bring any new information.

The new Krylov-based formulation of **FMR** provides an easy and more effective way to determine an appropriate value of  $r$ . We will simply monitor the rank of  $\mathbf{V}$  and will use this information as a stopping criterion *without computing*  $\mathbf{V}$ . There are two possible ways to achieve this goal. The first one is simply to use the diagonal entries of  $\mathbf{R}$  as a measure for the rank deficiency of  $\mathbf{V}$ . Note that  $\mathbf{R}$  is obtained iteratively at each step. Once the ratio  $\frac{\mathbf{R}(1,1)}{\mathbf{R}(k,k)}$  drops under certain tolerance, one can deduce that  $\mathbf{V}$  is rank deficient and the reduced model will not be improved with an additional step since no new information will be added to  $\mathbf{V}$ . The second way is to monitor the condition number of  $\mathbf{V}$ , which is equal to the condition number of  $\mathbf{R}$ , by computing the singular value decomposition of  $\mathbf{R}$  and examining the ratio

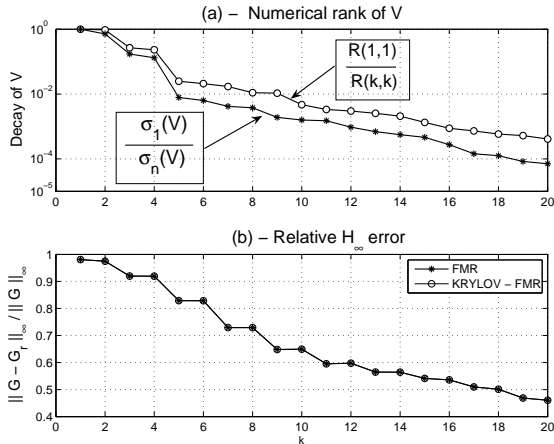


Fig. 1. **FMR** vs **RK-FMR** for  $\omega_0 = 300$

$\frac{\sigma_1(\mathbf{R})}{\sigma_k(\mathbf{R})}$ . Once this number is below a tolerance value, one can terminate the algorithm. We note that at the  $k^{\text{th}}$  step,  $\mathbf{R}$  has dimension  $k \times k$ , where  $k$  is small; hence SVD of  $\mathbf{R}$  is cheap. However, one still does not need to re-compute the SVD of  $\mathbf{R}$  at each step. The SVD of  $\mathbf{R}$  at the  $(k+1)^{\text{th}}$  step can be effectively updated using the SVD of  $\mathbf{R}$  from the  $k^{\text{th}}$  step since each step corresponds adding one column to  $\mathbf{R}$ ; see, for example, [13].

## 6 Numerical Example

In this section, we illustrate the concepts of Section 5 by a numerical example. The full-order model we use describes the dynamics between the lens actuator and the radial arm position of a portable CD player; it has 120 states, i.e.,  $n=120$ , with a single input and a single output. For more details on this system, see [2,9].

We apply the original formulation of **FMR** and the new rational Krylov formulation, denoted by **RK-FMR**, with the frequency  $\omega_0 = 300$  rad/sec and reduce the order to  $k = 1 : 20$ . The results are shown in Figures 1-(a) and 1-(b). Fig. 1-(a) depicts how the two ratios  $\frac{\mathbf{R}(1,1)}{\mathbf{R}(k,k)}$  and  $\frac{\sigma_1(\mathbf{V})}{\sigma_k(\mathbf{V})}$  evolve as  $k$  increases. The figure reveals that the ratio  $\frac{\mathbf{R}(1,1)}{\mathbf{R}(k,k)}$  follows the behavior of the true condition number quite well. Moreover, even for  $k = 20$ , the Krylov subspace  $\mathbf{V}$  is full-rank, which, in turn, implies that every iteration step brings in new information. This can also be seen in Fig. 1-(b) which shows that the  $\mathcal{H}_\infty$  error is reduced after each step, i.e. the reduced model is improved at each step. On the other hand, as Fig. 1-(b) illustrates, **RK-FMR** produces the same result as **FMR** without explicit moment computation.

For the second case, we apply **FMR** and **RK-FMR** with the frequency  $\omega_0 = 1.5$  rad/sec and reduce the order to  $k = 1 : 20$  as above. The evolution of  $\frac{\mathbf{R}(1,1)}{\mathbf{R}(k,k)}$  and

$\frac{\sigma_1(\mathbf{V})}{\sigma_k(\mathbf{V})}$ , and the relative  $\mathcal{H}_\infty$  error are depicted in Figures 2-(a) and (b), respectively. As Fig. 2-(a) illustrates, for this choice of  $\omega_0$ , the Krylov subspace  $\mathbf{V}$  becomes numerically rank deficient after a small number of iterations. Once more, the ratio  $\frac{\mathbf{R}(1,1)}{\mathbf{R}(k,k)}$  predicts the behavior of true condition number well. We set a tolerance value as  $\epsilon = 10^{-10}$  and terminate **RK-FMR** once  $\frac{\mathbf{R}(1,1)}{\mathbf{R}(k,k)}$  is below  $\epsilon$ ; this is the reason why the graph of  $\frac{\mathbf{R}(1,1)}{\mathbf{R}(k,k)}$  stays constant after  $k = 9$  (since no more steps are taken in **RK-FMR**). However, as Fig 2-(b) reveals there is almost no loss of accuracy in terms of the  $\mathcal{H}_\infty$  norm of the error. Since  $\mathbf{V}$  becomes almost rank-deficient, running **FMR** after  $k = 9$  barely improves the quality of the resulting error system. As can be seen from Fig. 2-(b), with  $k = 9$ , **RK-FMR** yields a relative  $\mathcal{H}_\infty$  error of 0.9997, while **FMR** with  $k = 20$  results in 0.9995. This indicates that, as expected from the conditioning of the Krylov subspace  $\mathbf{V}$ , almost no improvement has occurred despite increasing the reduced model size from  $k = 9$  to  $k = 20$ .

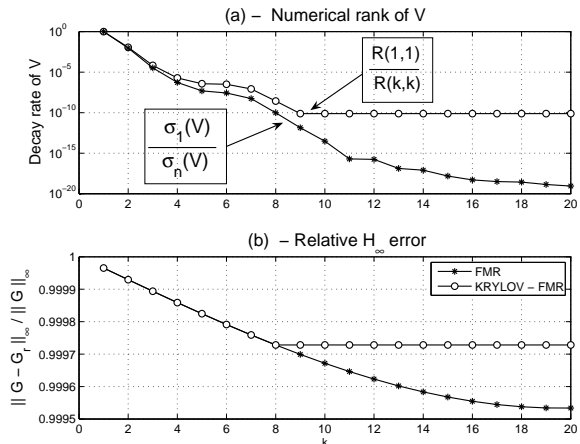


Fig. 2. **FMR** vs **Krylov-FMR** for  $\omega_0 = 1.5$

Finally, we examine if the behavior of  $\mathbf{V}$  for the second case, i.e. for  $\omega_0 = 1.5$ , can be recovered from inspecting the Markov parameters  $\eta_i$  of  $\mathbf{H}(z)$ ; in other words, we examine if magnitudes of  $\eta_i$  would be a reasonable stopping criterion. Figure 3 plots the Markov parameters  $\eta_i$  of  $\mathbf{H}(z)$  for  $\omega_0 = 1.5$  and shows that the  $\eta_i$  do not decay at all; on the contrary, they grow even until  $k = 40$ . This means that a stopping criterion based on the decay of  $\eta_i$  will yield unnecessarily large reduced order, even though this does not improve the quality of the reduced-order model as shown in Fig. 2-(b) above. Hence, the Krylov-based stopping criterion is more appropriate and numerically effective for **FMR**. Moreover, monitoring the rank of  $\mathbf{V}$  as done in **RK-FMR** can also be used to determine if the choice of  $\omega_0$  is poor at a much earlier stage. In this case, simply looking at the  $\mathcal{H}_\infty$  error behavior in Fig. 2-(b) and the decay of  $\eta_i$  in Fig. 3, one might decide to continue the **FMR** steps expecting that the error will

decay. However, monitoring  $\frac{\sigma_1(\mathbf{V})}{\sigma_k(\mathbf{V})}$  as in Fig. 2-(a) reveals that the subspace has become rank-deficient, and that the next step will not bring in new information; hence one should choose a different frequency  $\omega_0$ .

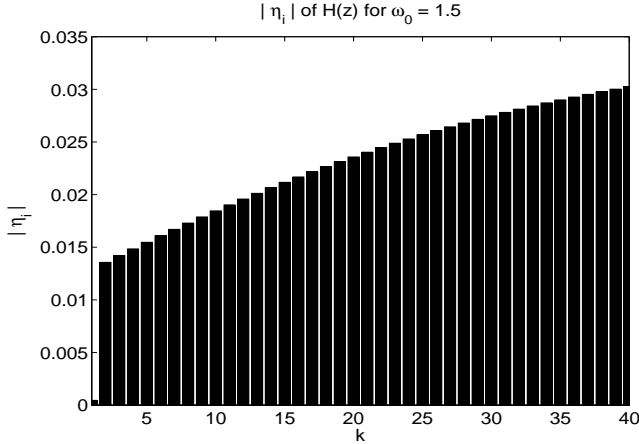


Fig. 3. FMR vs Krylov-FMR for  $\omega_0 = 1.5$

## 7 Conclusions

In this note, we have developed the rational Krylov projection framework for **FMR**, and introduced its interpolation and optimality properties. A numerically efficient Krylov-based setting has been illustrated to perform **FMR** and a new, more robust stopping criterion has been proposed.

## Acknowledgements

The work of S. Gugercin was supported in part by the NSF through Grants DMS-050597 and DMS-0513542; and the AFOSR through Grant FA9550-05-1-0449. The work of K. Willcox was supported in part by the Singapore-MIT Alliance Computational Engineering programme.

## References

- [1] V.M. Adamjan, D.Z. Arov, and M.G. Krein. Analytic Properties of Schmidt Pairs for a Hankel Operator and the Generalized Schur-Takagi Problem. *Math. USSR Sbornik*, 15:31–73, 1971.
- [2] A.C. Antoulas, D.C. Sorensen, and S. Gugercin. A survey of model reduction methods for large scale systems. *Contemporary Mathematics, AMS Publications*, 280:193–219, 2001.
- [3] M. Bettayeb, L.M. Silverman, and M.G. Safonov. Optimal Approximation of Continuous-Time Systems. *Proceedings of the 19th IEEE Conference on Decision and Control*, 1, December 1980.
- [4] C. De Villemagne and R.E. Skelton. Model reduction using a projection formulation. *International Jour. of Control*, 40:2141–2169, 1987.

- [5] P. Feldmann and R.W. Freund. Efficient Linear Circuit Analysis by Padé Approximation via the Lanczos Process. *IEEE Transactions on Computer-Aided Design of Integrated Circuits and Systems*, 14:639–649, 1995.
- [6] D. Gaier. *Lectures on Complex Approximation*. Birkhauser, 1987.
- [7] K. Gallivan, E. Grimme, and P. Van Dooren. Padé Approximation of Large-Scale Dynamic Systems with Lanczos Methods. *Proceedings of the 33rd IEEE Conference on Decision and Control*, December 1994.
- [8] K Glover. All Optimal Hankel-norm Approximations of Linear Multivariable Systems and their  $L^\infty$ -error Bounds. *International Journal of Control*, 39:1115–1193, 1984.
- [9] E. Grimme. *Krylov Projection Methods for Model Reduction*. PhD thesis, Coordinated-Science Laboratory, University of Illinois at Urbana-Champaign, 1997.
- [10] E.J. Grimme, D.C. Sorensen, and P. Van Dooren. Model reduction of state space systems via an implicitly restarted Lanczos method. *Numerical Algorithms*, 12:1–31, 1995.
- [11] S. Gugercin and A. Antoulas. A survey of model reduction by balanced truncation and some new results. *International Journal of Control*, 77:748–766, 2004.
- [12] S. Gugercin and A.C. Antoulas. Model reduction of large scale systems by least squares. *Linear Algebra and its Applications*, 415:290–321, 2006.
- [13] S. Gugercin, D.C. Sorensen, and A.C. Antoulas. A modified low-rank Smith method for large-scale Lyapunov Equations. *Numerical Algorithms*, 32:27–55, 2003.
- [14] P. Holmes, J.L. Lumley, and G. Berkooz. *Turbulence, Coherent Structures, Dynamical Systems and Symmetry*. Cambridge University Press, Cambridge, UK, 1996.
- [15] S-Y. Kung and D.W. Lin. Optimal Hankel-Norm Model Reductions: Multivariable Systems. *IEEE Transactions on Automatic Control*, AC-26(1):832–52, August 1981.
- [16] K. Kunisch and S. Volkwein. Control of Burgers’ equation by reduced order approach using proper orthogonal decomposition. *Journal of Optimization Theory and Applications*, 102:345–371, 1999.
- [17] J. Li and J. White. Low rank solution of Lyapunov equations. *SIAM Journal on Matrix Analysis and Applications*, 24(1):260–280, 2002.
- [18] L. Meier and D.G Luenberger. Approximation of Linear Constant Systems. *IEE. Trans. Automat. Contr.*, 12:585–588, 1967.
- [19] B.C. Moore. Principal Component Analysis in Linear Systems: Controllability, Observability, and Model Reduction. *IEEE Transactions on Automatic Control*, AC-26(1):17–31, August 1981.
- [20] C.T Mullis and R.A. Roberts. Synthesis of minimum roundoff noise fixed point digital filters. *IEEE Trans. on Circuits and Systems*, 23:551–562, 1976.
- [21] A. Ruhe. Rational Krylov algorithms for nonsymmetric eigenvalue problems II: matrix pair. *Linear Alg. Appl.*, 197:282–295, 1994.
- [22] L. Sirovich. Turbulence and the Dynamics of Coherent Structures. Part 1 : Coherent Structures. *Quarterly of Applied Mathematics*, 45(3):561–571, October 1987.
- [23] K. Willcox and A. Megretski. Fourier series for accurate, stable, reduced-order models in large-scale applications. *SIAM J. Scientific Computing*, 26(3):944–962, 2005.
- [24] A. Yousouff, D.A. Wagie, and R. Skelton. Linear system approximation via covariance equivalent realizations. *Journal of Math. Anal. and App.*, 196:91–115, 1985.